

tion methods have become most popular. These are the: (1) Latin Hypercube Simulation (LHS) [15,16] and (2) Markov Chain-Based Simulations (MCS) [17,18]. Although very efficient for finding the mean and standard deviation of the structural response, LHS loses its advantages when sampling the tails of the distributions which are needed when evaluating the probability of system failure. Even though they may require more sophisticated programming routines, Markov Chain-based simulations such as the Subset Simulation (SubSim) and variations on the method such as the Regenerative Adaptive Subset Simulation (RASS) are, in certain cases, emerging as viable alternatives to MCS and LHS methods [17,19].

The basic concept behind the Subset Simulation (SubSim) approach centers on the fact that a small probability of failure can be expressed as a product of large values of conditional failure probabilities by introducing several intermediate failure events. If F denotes the target failure region and $F_1 \supset \dots \supset F_i \supset \dots \supset F_m = F$ form a decreasing sequence of failure events, then:

$$P(C) = P(F_m/F_{m-1})P(F_{m-1}) = P(F_1) \prod_{i=2}^m P(F_i/F_{i-1}) \quad (2)$$

Eq. (2) shows that instead of calculating $P(C)$ directly, it can be calculated as the product of several conditional probabilities. With a proper choice of the conditional events, the conditional failure probabilities can be made sufficiently large so that they can be estimated using a small number of samples. Thus, the Subset Simulation avoids generating rare failure events to find small failure probabilities; instead it converts a problem involving rare events into a sequence of problems involving more frequent events [17]. Miao and Ghosn [19] introduced a number of modifications to further improve the subset simulation's accuracy, efficiency and its ability to handle structural systems with complex failure regions, large numbers of random variables, and small probabilities of failure.

A very simple example is solved by Miao [20] to demonstrate the validity and stability of the modified subset simulation method referred to as Regenerative Adaptive Subset Simulation (RASS). This example consists of a simplified bridge model formed by two parallel girders and two continuous spans as shown in Fig. 1. Assuming plastic behavior, two different failure modes

representing two different collapse mechanisms are possible. Each collapse mechanism can be modeled by a Limit State Function, Z_i , which can be written as:

$$Z_1 = 2(M_1 - D_1) + (M_2 - D_2) - \frac{P \times L_1}{2} \quad (3)$$

$$Z_2 = 2(M_3 - D_3) + (M_2 - D_2) - \frac{P \times L_2}{2} \quad (4)$$

where M_i is the moment capacity at section i , D_i is the dead load moment at section i , P is the applied maximum lifetime truck load, and L_j is the length of span j . The concentrated load P is used to model the weight of a nominal design truck (320 kN) with a dynamic amplification factor equal to 1.15 and a load distribution factor equal to 0.5 assuming the bridge is formed by two parallel beams each carrying half the total load. Table 1 gives the properties of the random variables. The reliability analysis is performed using MCS, SubSim and RASS for each failure mode separately and for the entire system. Table 2 lists the reliability index and the probability of failure for each mode and the probability of failure of the system as well as the number of runs needed to achieve convergence. The reliability index values listed in Table 2 for each method are the average values based on 50 independent analyses. For the analyses using SubSim and MCS the number of runs reflects the average number from the 50 simulations necessary to achieve convergence. For RASS, the number of runs was selected so that the COV (coefficient of variation) of the calculated probability of failure is the same as that obtained when using SubSim. Table 2 shows how both SubSim and RASS are significantly more efficient than MCS with RASS giving slightly more accurate results compared to MCS with close to 20% fewer analysis runs than SubSim.

3. Progressive collapse analysis methodology

Modeling techniques for progressive collapse analysis range from simple two-dimensional linear-elastic static procedures to very complex three-dimensional, nonlinear time history dynamic analyses. In this study, the progressive collapse analysis process is modeled by instantaneously applying ramped up reaction loads equal and opposite to those that were originally applied on the damaged element before damage took place. Thus, an impulsive dynamic load is applied to the structure that is held in its initial, undamaged position by the application of the reaction loads. Fig. 2 shows a schematic representation outlining the dynamic analysis process on the model of a truss bridge following the approach outlined by Buscemi & Marjanishvili [2]. Specifically, the progressive collapse analysis using the instantaneously applied load technique follows these steps:

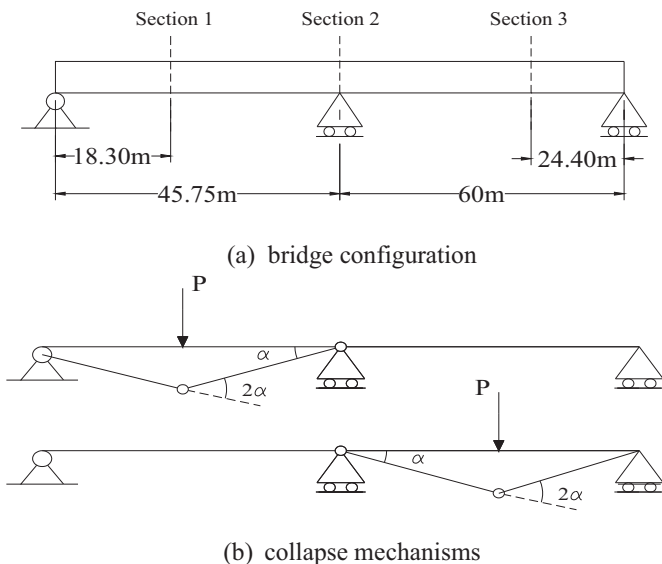


Fig. 1. Simplified two-span, two-girder continuous bridge configuration.

Table 1
Random variables for simplified two-span two-girder continuous bridge example.

	Variable	Nominal value	Bias	COV	Distribution type
Section 1	Moment Cap. (kN-m)	8190	1.12	10%	Lognormal
	Dead Load (kN-m)	3640	1.05	9%	Normal
	Live Load (kN)	320	2.07	19%	Extreme I
Section 2	Moment Cap. (kN-m)	23,400	1.12	10%	Lognormal
	Dead Load (kN-m)	13,755	1.05	9%	Normal
	Live Load	NA	NA	NA	NA
Section 3	Moment Cap. (kN-m)	19,217	1.12	10%	Lognormal
	Dead Load (kN-m)	10,750	1.05	9%	Normal
	Live Load	320	2.07	19%	Extreme I

Table 2
Comparison of results for simplified two-span two-girder continuous bridge example.

Simulation method	Reliability index for Z_1	Reliability index for Z_2	Probability of failure for Z_1	Probability of failure for Z_2	Probability of system failure
Original SubSim	3.75 (6830 runs)	3.75 (7326 runs)	8.74×10^{-5}	8.86×10^{-5}	1.75×10^{-4} (12,272 runs)
Proposed RASS	3.69 (5420 runs)	3.71 (6096 runs)	1.13×10^{-4}	1.04×10^{-4}	2.12×10^{-4} (10,072 runs)
Monte Carlo	3.71 (3.3×10^6 runs)	3.73 (3.5×10^6 runs)	1.04×10^{-4}	9.57×10^{-5}	2.06×10^{-4} (6.4×10^6 runs)

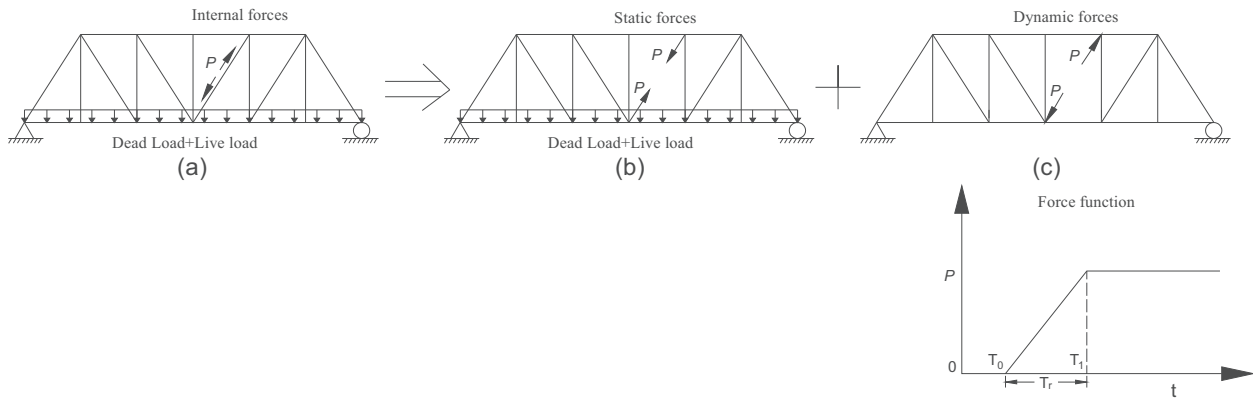


Fig. 2. Progressive collapse analysis process.

1. Perform a static analysis to determine the internal forces in the load bearing element to be removed. As an example, in the truss shown in Fig. 2a, one of the diagonal struts is assumed to be the element that will be subjected to sudden damage. The internal force in the member is equal to P .
2. Change the structural geometry by removing the load bearing element that will be damaged as shown in Fig. 2b and replace it by the internal force P calculated in step 1.
3. Apply on the system a sudden a dynamic force equal and opposite to P over a short impulsive time duration T_r as shown in Fig. 2c. When the system's dynamic response is dominated by one main vibration mode, it is commonly recommended to choose T_r be 1/10 times the first natural period of the structural system. In this paper, different values of T_r are investigated to compare the results as discussed further below.
4. Evaluate the dynamic response due to the sudden application of the impulsive force to check whether collapse occurs.

In this paper, the progressive collapse analysis is applied to structural models of two typical bridge configurations. The first bridge is a composite steel two-box girder bridge that may be subject to sudden failure as the result of fatigue crack propagation in one of the boxes. The second bridge is a steel truss bridge that may lose one of its members due to a collision. These two bridge types are selected for this investigation because, according to the US Federal Highway Administration (FHWA) definitions, they are classified as non-redundant configurations that would collapse if one member is fractured [21]. Sections 4–6 give short descriptions of the structural models and random variables for the bridges selected for investigation.

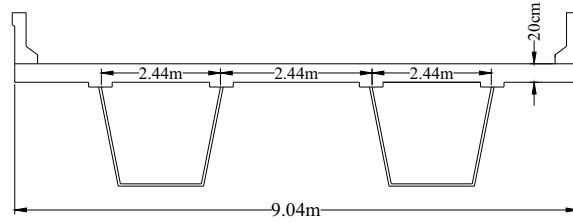
4. Structural model of box-girder bridge

According to FHWA and American Association of State Highway and Transportation Officials, AASHTO [21] criteria, steel two-box girder bridges are considered to be fracture critical, meaning that if a fatigue crack is initiated and propagates in one of the two boxes, the system will collapse. One goal of this study is to assess

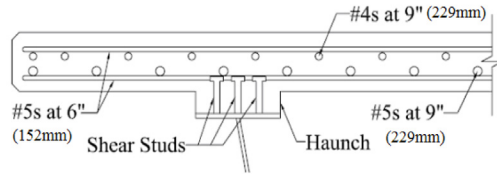
the ability of a box-girder system to survive the fracture process and the associated release of energy.

The progressive collapse analysis process is described using the model of a 36.6 m-long (120 ft) and 7.2 m wide (23 ft–8 in.) steel box-girder bridge having the cross section shape shown in Fig. 3a. The concrete deck thickness is 200 mm (8 in.) with a 75 mm (3 in.) haunch over each flange. The concrete deck is reinforced with two layers of rebars placed transversely and longitudinally. The rebar profile can be found in Fig. 3b based on an actual deck design provided by Hovell [22]. The bridge longitudinal members are designed following the current AASHTO LRFD specifications [21] to yield member reliability index values $\beta_{member} = 3.5$. For the analysis, the structure is modeled as a grillage with longitudinal members ($L1$) representing the composite properties of $1/2$ of the box (Fig. 3c). The transverse members, $S1$, represent the transverse properties of the slab. Transverse members $T1$ represent the transverse properties of the section enclosed by the box. Members $C1$ represent the sections that are prone to fracture. A 15.2 cm (6 in.) fracture is assumed to cut all the way through the entire width of the bottom flange and propagate through the two webs of a box whose capacity would be reduced to that of the 20 cm (8 in.) slab only. Table 3 lists the nominal member properties. The nonlinear behavior of the members is represented by moment–curvature relationships similar to the one shown in Fig. 3c for the longitudinal members and the one shown in Fig. 3d for the transverse slab members. The maximum curvature is obtained through section analysis based on section dimensions and material properties, such as stress and strain relationships for concrete, reinforcing steel and structural steel. To obtain the maximum plastic rotation, the maximum curvature is multiplied by a plastic hinge length L_p equal to the depth of the section as long as the depth is less than half the beam element length. Otherwise, half the element length is used for L_p . The selection of the plastic hinge length was based on comparisons with results of field tests available in the literature as described by Miao [20].

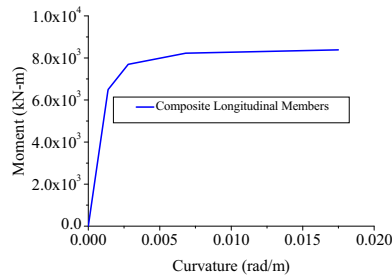
The nominal resistance values for bridge members are usually on the conservative side. Nowak [23] assumes that the member resistances can be modeled by lognormal probability distributions where the mean and Coefficient Of Variation (COV) of the moment capacities are related to the nominal values by a bias equal to 1.12



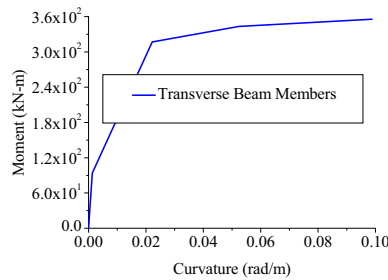
(a) Cross section of box-girder bridge



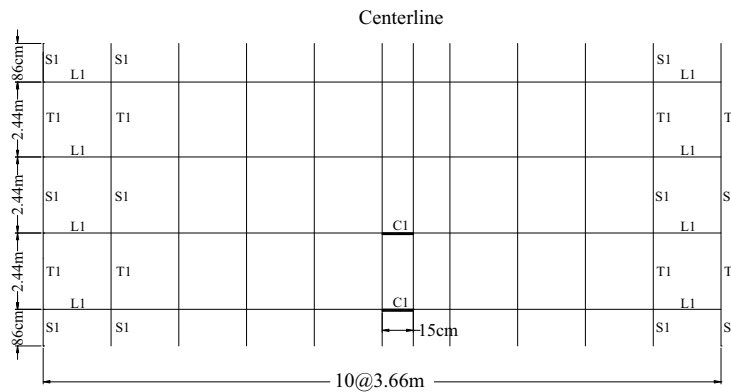
(b) Rebar profile in cast-in-place concrete deck based on [22]



(c) Moment-curvature for composite longitudinal beams



(d) Moment-curvature for transverse slab beam elements



(e) Grillage model of fractured bridge

Fig. 3. Model of steel two-box girder bridge.

and a COV of 10% for composite steel beams and a bias of 1.14 and a COV = 13% for reinforced concrete beams. In this study, the same

biases and COV values recommended by Nowak [23] are applied on the entire moment–curvature relationships used in the grillage

Table 3
Properties of steel two-box girder bridge members.

	Moment of inertia, I , (cm^4) (in^4)	Torsional constant, J , (cm^4) (in^4)	Nominal moment capacity (kN-m) (Kip-in)
Composite longitudinal beams ($L1$)	3.4×10^6 (82,182)	7.2×10^5 (17,248)	8400 (74370.5)
Cracked longitudinal beams ($C1$)	1.3×10^5 (3122)	2.6×10^5 (6144)	172 (1519.5)
Transverse box beams ($T1$)	1.1×10^7 (261,304)	3.9×10^7 (932,279)	19,815 (175,365)
Transverse slab beams ($S1$)	2.6×10^5 (6144)	5.1×10^5 (12,288)	343 (3039)

model. Members of the same type are conservatively assumed to be fully correlated such that all longitudinal members keep the same properties in each realization during the simulations and the same is true for the transverse beams. However, the longitudinal member properties are assumed to be statistically independent of those of the transverse members. These assumptions which are commonly made are reasonable based on bridge construction practices where steel members are normally manufactured in the same plant and concrete decks are formed on site using consistent procedures.

The dead loads, representing the weight of the steel box taken as $W1 = 3.15 \text{ kN/m}$ (0.018 kip/in), along with the weight of the concrete deck $W2 = 12.43 \text{ kN/m}$ (0.071 kip/in), and the weight due to the guardrail $W3 = 2.45 \text{ kN/m}$ (0.014 kips/in), are applied on the longitudinal beam elements. The dead loads are assumed to follow normal probability distributions with a bias of 1.05 and a COV of 10%.

The grillage model is commonly used for analyzing all types of deck on girder bridges (see for example [24,13,25]) and has been adopted in this study because of its simplicity. The model has been found to give good results when compared to more advanced analysis methods and experimental load deformation curves [20,26].

5. Structural model of steel truss bridge

Following the collapse of the I-35 Bridge in Minnesota, there has been renewed interest in evaluating the redundancy of truss bridges and their ability to withstand local failures [27]. However, there is no consensus among bridge engineers on the type of analyses that should be implemented and on the acceptability criteria that should be specified. In this study, a truss bridge is used as an example to demonstrate how the results of a probabilistic progressive collapse analysis can be used to develop incremental analysis criteria that can be implemented in engineering practice.

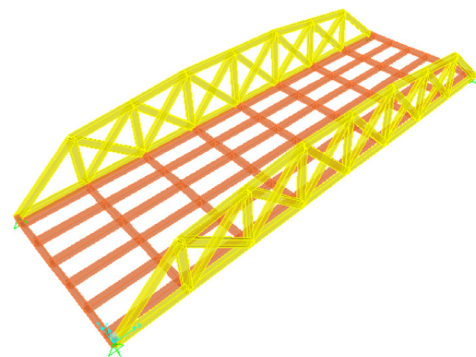
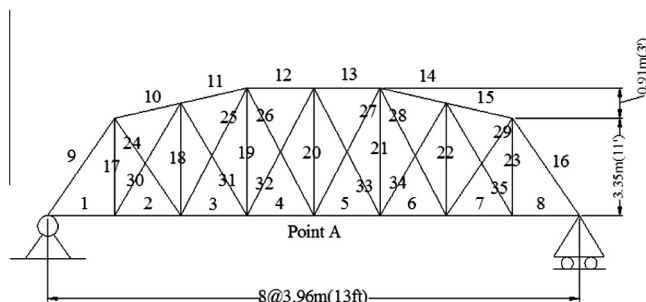


Fig. 4. Layout of steel truss bridge.

The through-truss bridge analyzed has two identical parallel trusses having the configuration shown in Fig. 4. The two parallel trusses are connected by cross beams supporting a concrete deck. The concrete deck is 178 mm (7 in.) thick and 10.36 m (408 in.) wide. The probabilistic models adapted for evaluating the reliability of this bridge, including the models for loads and structural members, and the execution of the probabilistic analysis of the system are consistent with those typically used during the reliability-based calibration of structural codes and standards as described in many references including [10,12,23,25,28].

The nominal dead weights are obtained as 31.52 kN/m (0.18 kip/in) assuming they follow a normal probability distribution associated with a bias = 1.05 and a COV = 10%. The structural model includes the main struts and the connections, which consist of the bolts and gusset plates. The bridge main members are designed to produce a member reliability index $\beta_{member} = 3.5$. Table 4 gives a listing of the truss Grade 36 (248 MPa) members' cross sectional areas. The Grade 36 gusset plates were generally 101.6 cm \times 101.6 cm \times 1.27 cm (40 in. \times 40 in. \times 0.5 in.) except for the middle section of the bridge which required plates that were 1.59 cm (0.625 in.) thick. The 25 mm (1 in.) diameter bolts having $2.4 \times 10^5 \text{ kPa}$ (35 ksi) shearing capacity are used to connect the members to the gusset plates. The top and bottom chords have 6 sets of fasteners arranged in rows of 4 bolts each. The diagonals required 5 sets of 4-bolt rows while the verticals were designed using 5 sets with 2 bolts in each row.

5.1. Material Properties

Fig. 5 and Table 5 show the nonlinear stress–strain model used for steel strut members as collected from several references. The statistical properties of the strain at ultimate, ϵ_u , are inferred from Fig. 5 given the data for the other parameters listed in Table 5. The upper range for the plastic strain is set at $\epsilon_p = 15 \epsilon_y$ based on experimental data collected by Miao [20].

Based on collected data from the literature [35–39], a tri-linear shear stress–deformation model is used to describe the behavior of A325 bolts as shown in Fig. 6 and Table 6. An additional reduction factor of 0.80 is applied to account for the non-uniform distribution of load between fasteners when the joint length is on the order of 76.2 cm (30 in.).

Based on data provided by Rex and Easterling [40] and Kim and Yura [41], a bilinear force–displacement model for the bearing capacity of gusset plates is developed as shown in Fig. 7, where the ultimate deformation, Δ_2 , is a function of the distance between the edge of the plate and the bolt, L_e , the ultimate strength of the steel, F_u , and the diameter of the bolts d_b . A regression analysis is performed to give the following relationship between Δ_2 (mm), L_e (mm), F_u (kN/mm) and d_b (mm).

Table 4
Truss member cross sectional areas.

No.	Area (cm ²) (in ²)	No.	Area (cm ²) (in ²)	No.	Area (cm ²) (in ²)
1	90.32 (14.00)	13	113.48 (17.59)	25	11.87 (1.84)
2	96.32 (14.93)	14	104.77 (16.24)	26	23.74 (3.68)
3	111.10 (17.22)	15	72.32 (11.21)	27	23.74 (3.68)
4	121.61 (18.85)	16	68.97 (10.69)	28	11.87 (1.84)
5	121.61 (18.85)	17	26.32 (4.08)	29	41.16 (6.38)
6	111.10 (17.22)	18	5.61 (0.87)	30	12.77 (1.98)
7	96.32 (14.93)	19	15.87 (2.46)	31	17.10 (2.65)
8	90.32 (14.00)	20	1.23 (0.19)	32	3.55 (0.55)
9	68.97 (10.69)	21	15.87 (2.46)	33	3.55 (0.55)
10	72.32 (11.21)	22	5.61 (0.87)	34	17.10 (2.65)
11	104.77 (16.24)	23	26.32 (4.08)	35	12.77 (1.98)
12	113.48 (17.59)	24	41.16 (6.38)		

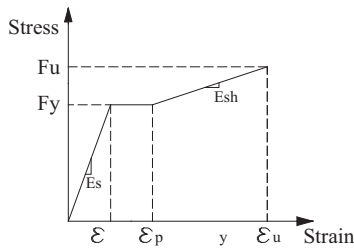


Fig. 5. Stress–strain relationship for steel truss members.

Table 5
Statistics of random variables for steel truss members.

Random variable	Nominal	Bias	COV	distribution type	References
F_y	2.48×10^5 kPa (36 ksi)	1.10	11%	Log-normal	[28,29]
F_u	4.00×10^5 kPa (58 ksi)	1.10	11%	Log-normal	[28,29]
E_s	2.00×10^8 kPa (29,000 ksi)	1.08	6%	Normal	[30–32]
E_{sh}	4.14×10^6 kPa (600 ksi)	1.00	25%	Normal	[33,34]

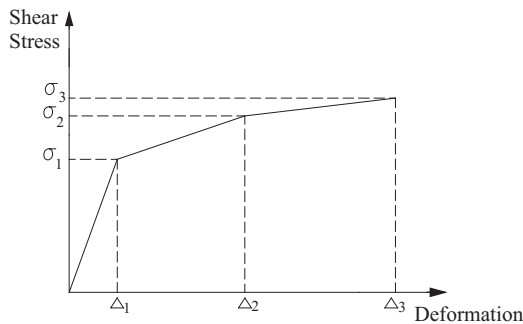


Fig. 6. Shearing stress–strain relationship for fasteners.

$$\Delta_2 = -7.9462 + 1.1315 \times L_e - 0.0129 \times F_u + 0.1331 \times d_b - 0.0137 \times L_e^2 \quad (5)$$

Δ_1 is taken to be $\frac{1}{6}\Delta_2$. The initial stiffness, K_i , is estimated using the model provided by [40].

$$K_i = \frac{1}{\frac{1}{K_{br}} + \frac{1}{K_b} + \frac{1}{K_v}} \quad (6)$$

Table 6
Statistics of random variables for fasteners.

Random variable	Mean	COV	Distribution type	References
σ_1	2.85×10^5 kPa (41.30 ksi)	10%	Normal	[35–38]
σ_2	4.45×10^5 kPa (64.54 ksi)	10%	Normal	
σ_3	4.92×10^5 kPa (71.42 ksi)	10%	Normal	
Δ_1	0.091 cm (0.036 in.)	8%	Normal	
Δ_2	0.30 cm (0.12 in.)	8%	Normal	
Δ_3	0.58 cm (0.23 in.)	8%	Normal	

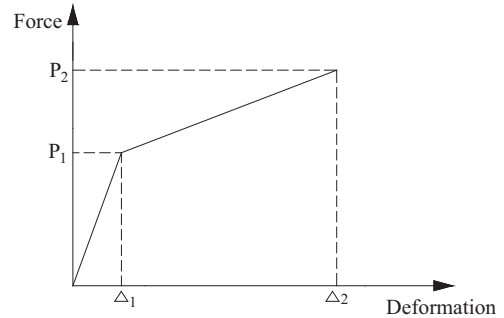


Fig. 7. Bilinear force–displacement model for bearing plates.

where the bearing stiffness is $K_{br} = 120t_p F_y (d_b/25.4)^{0.8}$; the bending stiffness is $K_b = 32Et_p (L_e/d_b - 1/2)^3$; and the shearing stiffness is $K_v = 6.67Gt_p (L_e/d_b - 1/2)$ in which G is shear modulus of elasticity and t_p is the plate thickness

P_1 can be found from Δ_1 and K_i . Also, given Δ_2 and K_i , P_2 can be obtained from Eq. (7) which is based on the model by Rex and Easterling [40].

$$\frac{P_2}{P_n} = \frac{1.74\bar{\Delta}}{(1 + \bar{\Delta}^{0.5})^2} - 0.009\bar{\Delta} \quad (7)$$

where P_2 = plate ultimate load carrying capacity; P_n = nominal plate strength; $\bar{\Delta}$ = normalized deformation = $\Delta K_i/P_n$; Δ = hole elongation; and K_i = initial stiffness.

The nominal capacity, P_n , is the product of the plate cross sectional area and the nominal strength, F_b , given by Fisher and Struik [42] as:

$$F_b = 1.2F_u \frac{L_e}{d_b} \leq 2.4F_u \quad (8)$$

The bias for the force versus displacement relationship is represented by a modeling random variable, γ_p , having a mean value = 1.05 with a COV = 5%. This bias is in addition to the biases and coefficients of variation for the material properties.

In addition to possible failures due to exceeding the ultimate capacities of the struts, fasteners or gusset plates, trusses are susceptible to buckling modes of failure. The nominal buckling stresses for struts under compressive axial loads can be obtained from the manual of the American Institute for Steel Construction [43] that gives the following equations:

$$\text{For } \frac{KL}{r} \leq 4.71 \sqrt{\frac{E}{QF_y}}, F_{cr} = \left[0.658 \frac{QF_y}{F_e} \right] QF_y \quad (9)$$

$$\text{For } \frac{KL}{r} > 4.71 \sqrt{\frac{E}{QF_y}}, F_{cr} = \frac{0.877\pi^2 E}{\left(\frac{KL}{r}\right)^2} \quad (10)$$

where F_{cr} is the buckling stress; F_y is the yielding stress; K = effective length factor; L = length of member; r = radius of gyration = $\sqrt{I/A_g}$; A_g = gross cross sectional area; I = moment of inertia; E = modulus of elasticity; $F_e = \frac{\pi^2 E}{(\frac{KL}{r})^2}$; Q = form factor to consider the reduction in efficiency of the cross section in accordance with AISC [43].

For plates in compression, the AISC (2010) buckling stress is given as:

$$F_{cr} = k \frac{\pi^2 E}{12(1 - \mu^2)(b/t)^2} \quad (11)$$

where k is a constant depending on the type of stress [44], edge support conditions, and length to width ratio (aspect ratio) of the plate, μ is Poisson's ratio, b/t is the width/thickness ratio.

Comparisons between Eqs. (9) and (10) and experimental data conducted by Hall [45] demonstrate that there is a modeling bias equal to 1.13 and a COV equal to 9%. Because no data is available to compare the buckling of gusset plates and the AISC (2010) equations adopted in Eq. (11), it is assumed that the bias = 1.13 and the COV = 9% are valid for both plate and strut buckling models.

6. Live load model

To perform the reliability analysis of bridge systems, it is necessary to have probabilistic models for the dead loads and the lives loads. As presented earlier, the dead load is assumed to follow a normal distribution with a bias equal to 1.05 and a COV = 10% based on Nowak's [23] recommendation. The live load model used in this analysis is based on Weigh-In-Motion (WIM) data collected at a representative site in Central New York State along the I-81 Corridor following the methodology developed by Ghosn et al. [46] and Sivakumar, Ghosn and Moses [47]. WIM data provides information on truck weights and arrival times which can be used to obtain the maximum expected load effects including those due to multiple truck presence on bridges for different design lives or service periods

Using the WIM data, the load effect of each truck loading event is calculated by passing the trucks through the proper influence line. The load effect of each set of trucks that are expected to be on the bridge simultaneously is then normalized by dividing the calculated value by the effect of a typical standard truck. The results are collected into frequency plots or cumulative distribution histograms, $F_{xs}(X_s)$, for a single lane of trucks or for trucks side by side on multi-lane bridges. For illustration, Fig. 8 shows in black squares the moment histogram for a single lane of trucks and in red diamonds the data from two lanes for a 30.48 m (100 ft) simple span bridge obtained from the data collected from the I-81 WIM site. The moments are normalized with respect to the moment

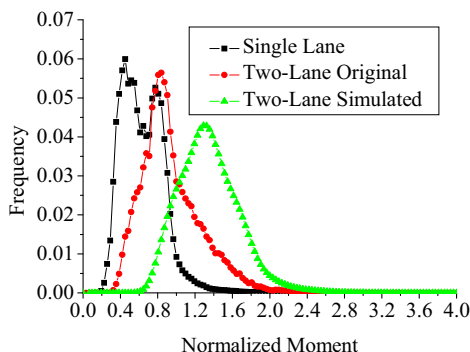


Fig. 8. Normalized truck load moment effect histogram for 30.48 m (100 ft) bridge.

effect of the AASHTO 3S2 semi-trailer Legal Truck having a total weight equal to 320 kN (72 kip) [48]. The Legal 3S2 truck represents typical semi-trailer trucks that meet the US federal legal limits for groups of axles and gross weights.

Because of the relatively limited set of data that is available and the low probability of side-by-side events, it has been common to use a simulation approach to obtain the load model for two-lane traffic. Assuming independence, the probability density function of the effect of side-by-side trucks on a two-lane bridge can be calculated using the convolution:

$$f_{xs}(X_s) = \int_{-\infty}^{+\infty} f_{x2}(X_s - x_1) f_{x1}(x_1) dx_1 \quad (12)$$

where $f_{xs}(\dots)$ is the probability distribution of the multi-lane effects, $f_{x1}(\dots)$ is the probability distribution of the effects of trucks in lane 1, $f_{x2}(\dots)$ is the probability distribution of the effects of trucks in lane 2. The total load effect can be set as $X_s = X_1 + X_2$ where X_1 is the effect of the trucks in the drive lane and X_2 is the effect those in the passing lane. It is assumed that $f_{x2}(\dots) = f_{x1}(\dots)$ based on the observation made by Sivakumar et al. [47] that the truck weight statistics in the passing lanes are similar but uncorrelated to those in the drive lane. Fig. 8 shows in green triangles the histogram obtained for the two-lane loading events obtained from Eq. (12). Compared to the two-lane loading histogram obtained directly from the WIM data shown in red, the convolution yields more conservative values due to the assumption that trucks in two lanes that are within 60-ft head to head are compressed so that they are placed side-by-side. Also, some additional conservatism is due to the assumption that the percentage of trucks closely following each other is the same in both lanes.

For a bridge structural system to be safe, the resistance should be large enough to withstand the maximum load effect that could occur within a pre-set service period. The design life of a new bridge is specified to be 75 years as per the AASHTO LRFD code [21]. A 5-year service period has been used for the load rating of existing bridges as specified in the AASHTO LRFR code [48]. Assuming independence between the various events, the cumulative probability distribution of the maximum load effect, LL , in a service period, T , during which N loading events are expected is obtained from:

$$F(LL) = F_{xs}(X_s)^N \quad (13)$$

where the number of events, N , is obtained from the WIM data based on the Average Daily Truck Traffic (ADTT) and the headways considering the number of multi-lane events and the location of the trucks relative to each other during such events. When N is very large, it is necessary to assume that the tail end of $F(LL)$ follows a known probability distribution. This will allow for extending the range of the WIM data beyond the upper range limits of the available data. In the work performed by Sivakumar et al. [47], it was determined that the upper 5% of the histogram's tail end approaches that of Normal probability distribution. Fig. 9 plots the cumulative probability distribution for the maximum two-lane live load obtained for a 36.58 m (120 ft) simple span for different service years. In Fig. 9 the live load effects are also normalized in terms of equivalent AASHTO 3S2 Legal Load truck [48]. The Legal truck, which unlike the AASHTO design load model has a configuration of a typical semi-trailer truck, is used because the nonlinear structural analysis requires the application of loads that resemble actual truck configurations. Note that although N is a random variable, the effect of changes in N on the cumulative distribution $F(LL)$ is relatively small when N is very large as is the case for live loads on highway bridges. The conservative load effect probability models obtained from the simulated side-by-side trucks are used for the bridges analyzed in this paper.

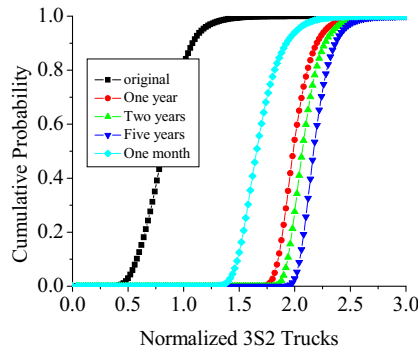


Fig. 9. Cumulative probability distribution of live load for 36.58 m (120-ft) bridge.

7. Probabilistic analysis of system redundancy, robustness and progressive collapse

Probabilistic analyses of the box girder bridge and the truss bridge described earlier are performed using RASS method described by Miao and Ghosn [19]. As explained in Section 2, the method is based on a Markov chain simulation process that calculates the probability of a structural system’s failure P_f . The reliability index is calculated as $\beta = \Phi^{-1}(-P_f)$, where Φ^{-1} is the inverse of the cumulative probability function of the standard normal distribution. Several analyses are performed to evaluate the reliability of: (a) main bridge members of each system; (b) each system in its originally intact configuration; (c) each system after major damage assumed to involve the loss in the load carrying capacity of one critical member; and (d) each system during the sudden loss of a main member. For case (a), the analysis assumes linear-elastic behavior and failure is defined as the point at which a main member reaches its load carrying capacity. This is done to remain consistent with the assumptions used during the calibration of the current AASHTO bridge design specifications [21,23]. For case (b), the reliability analysis accounts for the nonlinear behavior of the system and failure is defined as the point at which a main member fractures, crushes or buckles. When analyzing cases (c) and (d), the box girder bridge is assumed to have undergone a fatigue fracture that sliced through the bottom flange and the two webs of one box. Also, when analyzing cases (c) and (d), the truss bridge is assumed to have undergone damage or fracture to one main strut member. This damage could be due to fatigue fracture of tension members or vehicular impact. These damage scenarios are selected because the two bridge types being analyzed have been designated by the US Federal Highway Administration (FHWA) as non-redundant, fracture-critical configurations that are expected to collapse under their own weights if one of their members is fractured [21]. The reliability analyses undertaken for cases (a), (b), and (c) are based on the behavior under static loads. For case (d), a dynamic reliability analysis is performed.

The analyses performed in this paper seek to evaluate the ability of these bridge systems to continue to carry some level of service traffic load during and after damage takes place. In the context of this paper, structural redundancy is defined as the ability of the originally intact system to continue to carry load beyond the level at which the first member reaches its capacity. Structural robustness is defined as the ability of a bridge system in its damaged state to still be able to carry some level of service traffic load [26,49]. A bridge is said to be able to mitigate disproportionate collapse if it can sustain the dynamic release of energy associated with a sudden damage. Accordingly, probabilistic analyses are performed to determine the following:

1. The reliability index of the most critical member under the effect of the maximum 75-year load. This is done to compare whether the bridge designs selected for this analysis are consistent with the AASHTO LRFD safety criteria which were developed so that bridge designs achieve member reliability indexes $\beta_{member} = 3.5$.
2. The reliability of the originally intact system if subjected to the effect of the 75-year maximum live load. The purpose is to verify that the bridge’s structural system provides sufficiently high levels of reserve strength, ductility and redundancy to withstand a potential extreme live load beyond the load that causes first member failure. According to Ghosn and Moses [13], a typical bridge system should have a reliability index higher than that of its most critical member by at least $\Delta\beta_{ultimate} = \beta_{ultimate} - \beta_{member} = 0.85$ to be considered to have a sufficient level of structural redundancy.
3. The reliability of the bridge in a damaged state is studied to evaluate its ability to sustain a minimum level of loads if one member has completely lost its load carrying capacity due to deterioration or damage. This analysis scenario verifies the ability of the damaged system to continue to carry some load if the system survives the initial damage process. A five-year service period is selected to represent bridge inspection and bridge rating cycles. According to Ghosn and Moses [13], a typical bridge in a damaged configuration can be allowed to have a reliability index lower than that of its most critical member by less than $\Delta\beta_{damaged} = -2.70$ to be considered to be sufficiently structurally robust.
4. The dynamic reliability analysis of the damage process assumes that the critical member is dynamically removed at the same time when it is loaded by service live loads. Because there are no criteria to determine the appropriate service loads, a 1-month maximum load is used in this study. It is also noted that there are no established criteria for assessing whether a bridge has sufficient reliability to mitigate disproportionate collapse. Such criteria will have to be established in consultation with bridge owners and stakeholders based on risk assessment principles and cost-benefit analyses. However, lacking better information, it is herein assumed that a reliability $\Delta\beta_{progressive} = -2.70$ or higher is acceptable with the understanding that a service live load corresponding to only the 1-month maximum truck load will be on the bridge when the sudden removal of the member takes place.

In this paper, a damaged truss bridge system which has already lost the load carrying capacity of one member is considered to have collapsed if any of its remaining main members reaches its maximum tension force or buckles or if any of the connections fails. For the damaged box girder bridge, the damage system is assumed to have collapsed if the deck over the fractured section reaches its maximum plastic rotation (see Table 7).

Table 7
Statistics of random variables – plate strength.

Random variable	Nominal	Bias	COV	Distribution type	References
F_y	2.48×10^5 kPa (36 ksi)	1.10	11%	Log-normal	[28,29]
F_u	4.0×10^5 kPa (58 ksi)	1.10	11%	Log-normal	[28,29]
E_s	2.0×10^8 kPa (29,000 ksi)	1.08	6%	Normal	[28,29]
G	7.69×10^7 kPa (11,154 ksi)	1.08	6%	Normal	[40]
γ_p	1.0	1.05	5%	Normal	[40]

Table 8
Reliability indexes for bridge systems.

Bridge	Member	Originally intact system		Damaged system		Progressive collapse	
	β_{member}	$\beta_{ultimate}$	$\Delta\beta_{ultimate}$	$\beta_{damaged}$	$\Delta\beta_{damaged}$	$\beta_{progressive}$	$\Delta\beta_{progressive}$
Box girder	3.50	4.69	1.19	2.92	-0.58	2.46	-1.04
Truss	3.50	4.61	1.11	-0.67	-4.17	-2.05	-5.55
Acceptability criteria	3.50	4.35	0.85	0.80	-2.70	0.80	-2.70

The results of the reliability analysis are summarized in Table 8. The results show that the reliability index for the most critical member in both bridges is equal to the target $\beta_{member} = 3.5$. The system reliability indexes, $\beta_{ultimate}$ for both bridges are above 4.60. This indicates that both bridge systems in their original intact configurations show high levels of structural redundancy demonstrating that they possess sufficient ductility and reserve strength to sustain extreme live loads even after their most critical member reaches its limiting capacity.

For the box-girder bridge, the damage scenario assumes that a fracture occurs in the bottom flange and the two webs of one box at the middle of the span. A 152-mm (6 in.) fracture cuts all the way through the entire steel section but the slab is assumed to continue to carry load. In this damaged configuration, the bridge can still sustain sufficiently high levels of load to allow for the crossing of regular traffic with an acceptable level of reliability $\beta_{damaged} = 2.92$ until such time that the damage is detected and appropriate repair actions are undertaken. The same however, is not true for the truss bridge. If member 29 (or by symmetry member 24) of Fig. 4 is totally damaged, the bridge system will have a negative reliability index equal to $\beta_{damaged} = -0.67$ which indicates a high probability of collapse under regular traffic conditions should this damage scenario take place.

Finally, the probabilistic dynamic analysis is performed assuming that impulsive damages take place with a sudden release of the energy embedded in the damaged members. In this case, the reliability index for the box-girder bridge is found to be $\beta_{progressive} = 2.46$ which indicates a reasonable reliability that the bridge will be able to sustain the sudden fracture of the box under service loading conditions. On the other hand the sudden impulsive fracture of member 29 of the truss leads to a very low reliability index $\beta_{progressive} = -2.05$ which indicates an unacceptably high probability of progressive collapse. Even though the member and system reliabilities of the two bridges as shown in Table 8 are similar, the effect of damage on the truss bridge is more significant than that for the box girder bridge. In particular, the dynamic effects associated with the sudden removal of member 29 of the truss are especially critical based on the collapse criteria adopted in this study. This is because the design of the truss members is optimized to meet the minimum design standards represented by a reliability index $\beta_{member} = 3.5$. Bridges with different member capacities are investigated in Section 9. Therefore, when one member is removed the remaining members have little additional reserve strength to carry the load shed by the damaged member. This is especially true when the removal is sudden associated with a large dynamic amplification. For the box girder bridge, the optimized design means that the two boxes will have similar capacities even if the placement of the truck loads will produce a higher load on one of the boxes. This situation will allow for easier transfer of load from the damaged box to the undamaged box. In fact, when the bridge acts as a system, the load from the member that is failing (or damaged) is transferred to the less loaded (or undamaged) parallel beam through the slab. This has been confirmed through analytical studies as well as experimental investigations. Ghosn et al. [13,26] in NCHRP Reports and 776 compared results of exper-

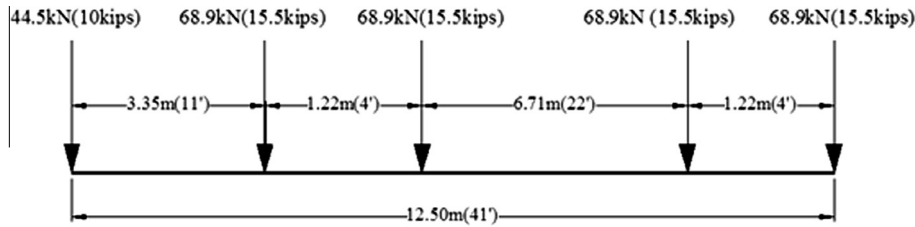
imental investigations to analytical results of full scale and laboratory scale bridge systems. They found that bridge decks designed to current standards have large abilities to sustain nonlinear behavior providing them with large capacities to transfer the loads laterally. The experimental work at the University of Texas Austin has also confirmed that two-box girder bridges can sustain high levels of loads due to the ability of slabs to transfer these loads laterally between the beams [22]. The main limitation appears to be related to the connection between the deck and the fractured steel members. Work on modeling the ability of the steel-concrete connections to transfer the loads in bridges with fractured boxes is in progress [50].

8. Calibration of load factors for use in incremental analysis

While the reliability analysis process described in Section 7 may be implementable by research engineers with appropriate training, the process is difficult to implement on a regular basis in bridge engineering practice. As an alternative, bridge engineers may follow an incremental nonlinear static analysis approach similar to that used for the evaluation of buildings using the GSA methodology if appropriate criteria are made available. This section describes how such criteria may be developed by bridge authorities and code writers.

For engineers to check the ability of a structure to mitigate disproportionate collapse using a nonlinear static analysis, they need to know what live loads to apply, and what appropriate load factors should be used. Following the GSA [6] and DOD [7] methods, the simplified analysis procedure must also explicitly consider nonlinear material behavior and implicitly account for the structural dynamic response by applying a dynamic amplification factor that will avoid the need to perform a structural dynamic analysis. Accordingly, checking the ability of a bridge structure to mitigate disproportionate collapse after a member is damaged may consist of the following steps: (a) develop a nonlinear finite element model for the bridge system; (b) Determine a possible damage scenario; (c) Remove the designated members corresponding to the damage scenario; (d) Apply the dead load without any safety factor; (e) apply a live load representing a typical truck configuration, for example, the 3S-2 AASHTO Legal Truck shown in Fig. 10; (f) Increment the live load and find the Incremental Load factor, ILF , that multiplies the 3S-2 load to cause bridge collapse; (g) Compare ILF to a specified ILF_{min} . If $ILF > ILF_{min}$, the bridge is considered to be sufficiently safe to sustain the designated damage scenario. Otherwise, the bridge is susceptible to progressive collapse and the bridge design should be modified by either increasing the capacities or the ductility of the members around the damage location to allow for the redistribution of the load or change the structure's topology to provide alternate load paths.

An outline of the reliability-based calibration procedure that code developers may follow to specify ILF_{min} may be summarized in the following 10 steps that the code writers need to expand on based on the types of bridges that the codes and standards are intended to address:



Type 3S2 unit weight=320 kN (72 kips)

Fig. 10. AASHTO Type 3S-2 truck configuration [48].

1. Assemble a representative sample of bridge configurations that may be susceptible to sudden damage from fracture, impact, collisions, blasts or other man-made or natural extreme events. The code writers and bridge owners should decide on the size of the sample and the types and dimensions covered to reflect the range of bridges that the guidelines intend to cover.
2. Initially, design the members of the intact structures following current member-oriented design standards. Update the design to cover a whole range of cases.
3. Perform dynamic reliability analyses of each system in the representative sample of bridges by removing one designated member suddenly and find $\beta_{progressive}$.
4. Perform a nonlinear incremental load analysis on the same structure analyzed in Step 3 after removing the same designated member. The analysis is performed by first applying the dead load and incrementing a representative truck configuration such as the AASHTO 3S-2 live load [48] [to find the ILF live load multiplier required to cause collapse. The total load that will be sustained will be designated as $D_n + ILF \times L_n$ where D_n is the nominal dead load and L_n is the 3S-2 Legal Truck.
5. Repeat steps 2–4 for each bridge after changing the bridge design.
6. Repeat steps 2–5 for different possible damage scenarios including the extent and location of damage that the code writers and bridge owners determine as relevant to the types of bridges considered and their exposure to damaging hazards.
7. Establish the relationships between the dynamic progressive collapse reliability index $\beta_{progressive}$ for each design and the Incremental Load Factor, ILF for different damage scenarios.
8. Based on risk evaluation and a cost-benefit analysis or bridge owner requirements, determine the acceptable level of reliability $\beta_{progressive}$ that can be tolerated and establish the corresponding ILF_{min} as the criterion for future evaluations of similar types of bridges under similar damage scenarios.
9. Ideally, the outcome of the calibration processes should be a limited set of ILF_{min} that will be applicable for most typical bridge configurations and damage scenarios. Such set of ILF_{min} criteria would then be suitable for implementation in appropriate bridge design specifications.
10. As a result of this calibration process, a bridge engineer will be able to decide which target ILF_{min} criterion a bridge design should satisfy in order to meet a given target reliability level. In this manner, the engineer can design a reliable system by simply performing an incremental nonlinear static analysis without the need to perform a dynamic reliability analysis.

The reliability calibration processes is illustrated for the two example bridges analyzed in this paper.

8.1. Box-girder bridge

Using the original design that produced a member reliability index $\beta_{member} = 3.5$, the dynamic probabilistic analysis is executed assuming that a fracture takes place at the mid-span of one box when the maximum 1-month live load is on the bridge and obtain the reliability index $\beta_{progressive} = 2.46$. With the same design, a nonlinear incremental analysis is executed to find that the Incremental Load Factor that causes collapse is $ILF = 1.8$. Subsequently, the capacity of all the longitudinal beams is multiplied by a factor of 0.8. The reliability index $\beta_{progressive} = 1.33$ and the corresponding $ILF = 1.53$ are obtained. By repeating the same procedure for different member capacities, the relationship between ILF and the reliability index $\beta_{progressive}$ is established as shown in Fig. 11.

The results in Fig. 11 help in selecting the appropriate incremental progressive analysis criteria that would meet a target reliability level. For example, if a reliability index $\beta_{progressive} = 2.00$ is required, then an engineer can simply execute a nonlinear incremental analysis of a fractured bridge and ensure that the damaged bridge will be able to carry its dead weight and 1.75 times the 3S-2 live load to be considered sufficiently safe. If a reliability index $\beta_{progressive} = 1.50$ is required, then the incremental load factor on the 3S2 truck should be $ILF = 1.67$. An $ILF = 1.54$ would correspond to a reliability index $\beta_{progressive} = 0.80$. These reliability indexes are those related to the conditional probability of collapse given the fatigue fracture of the one box of the two-box bridge $P(C|D)$. A reliability index $\beta_{progressive} = 0.80$ would lead to a conditional reliability $P(C|D) = 21.19\%$ if the bridge members are designed to meet a reliability index for fatigue fracture $\beta_{member} = 2.0$ or $P(D|H) = 2.28\%$ as intended by the AASHTO [21] specifications, then the unconditional probability of collapse will be 0.48% for a reliability index equal to 2.59. This value is similar to that allowed for the rating of existing bridges in the AASHTO MBE [48].

8.2. Truss bridge

The same type of analysis performed for the box-girder bridge is repeated for the truss bridge. Three damage scenarios are considered. Originally, all bridge members were designed to achieve a member reliability target $\beta_{member} = 3.5$. Subsequently the designs were adjusted to produce higher system reliabilities for the intact condition and several damage scenarios were investigated for each of the intact systems. The first scenario, $D1$, assumes that member 29 in Fig. 4 is dynamically removed. The second and third scenarios ($D2$ and $D3$) assume that member 23 and member 34 are suddenly removed, respectively. The results in Fig. 12 show different curves for each damage scenario. On the whole, the three curves lie within a reasonably narrow band but slightly shifted to the right of the curve of the box girder bridge in Fig. 11. The variations between the curves are due to the differences in the type of damages considered, the load path patterns, and live to dead load ratios of the two structural configurations and the damage scenarios.

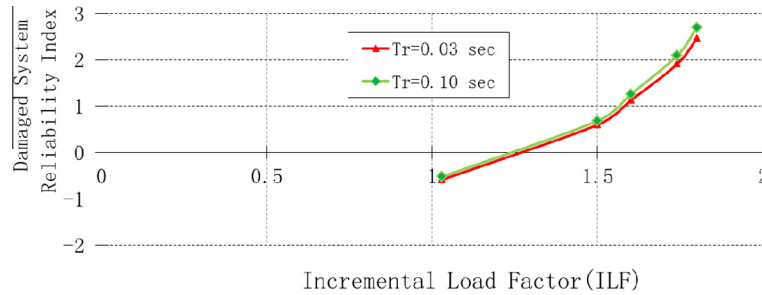


Fig. 11. Reliability index $\beta_{\text{progressive}}$ versus Incremental Load Factor ILF for box-girder bridge.

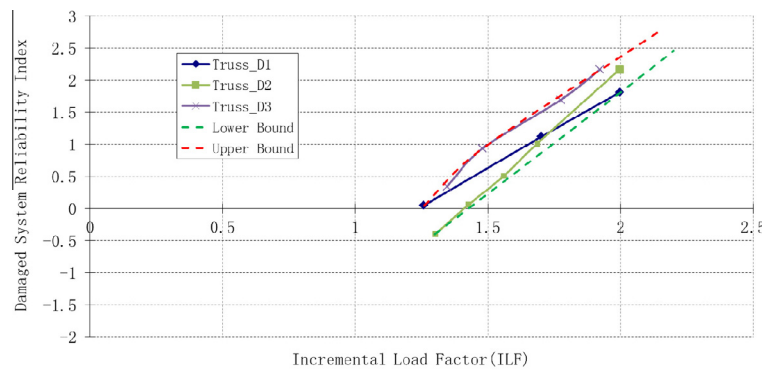


Fig. 12. Reliability index $\beta_{\text{progressive}}$ versus Incremental Load Factor ILF for different damage scenarios of truss bridge.

Fig. 12, indicates that if a target reliability index $\beta_{\text{progressive}} = 1.50$ is required, the incremental analysis of the damaged bridge should lead to a load carrying capacity equal to the bridge's dead weight plus somewhere between 1.67 and 1.83 times the 3S-2 live load. If the average value $ILF = 1.75$ is used, then the reliability index $\beta_{\text{progressive}}$ will fall between 1.25 and 1.75. Using $ILF = 1.83$ as a criterion for incremental analysis would be a conservative upper bound for this truss and damage scenarios considered. If a reliability index $\beta_{\text{progressive}} = 0.80$ is required, then the incremental load factor on the 3S2 truck should be between 1.45 and 1.63 with an average value $ILF = 1.55$ which is very similar to the value obtained for the box girder bridge for the same target reliability.

8.3. Effect of impulse time

Modeling the progressive collapse analysis process using the approach described in Fig. 2 requires the determination of the impulse rise time T_r . The actual time it takes a member to snap depends on the type of hazard that initiates the damage. A very short rupture time $T_r < 0.001$ s may represent damage scenarios associated with blast and fatigue crack propagation while values up to 1 s may represent rupture due to vehicle collisions. The effect of the impulse time on the results is also controlled by the time step Δt used during the nonlinear dynamic analysis. If $T_r < \Delta t$, the analysis is equivalent to an instantaneous removal of the damaged member which would lead to the most conservative results. A $\Delta t = 0.05$ s was selected for the dynamic reliability analysis which is higher than $T_r = 0.03$ s used for the analysis of the box girder and $T_r = 0.006$ s used for the truss bridge analysis. These values, both of which are less than $\Delta t = 0.05$ s were selected because they are approximately equal to 1/10 the dominant natural periods of each system. The effect of T_r on one realization of each bridge are presented in Fig. 13 which compares the results obtained for

$T_r = 0.002, 0.01, 0.05$ and 0.10 s. The figure clearly shows that when $T_r = 0.002$ or 0.01 s, the results are most conservative leading to the highest possible Incremental Load Factor, ILF , which in Fig. 13 are normalized to give a maximum value equal to 1.0. As T_r increases above $\Delta t = 0.05$ s, the error in ILF increases to about 8%. The sensitivity analysis also shows that this level of error is reduced during the probabilistic analysis as its effects on the final results are dampened by the large levels of uncertainties associated with the estimation of the applied loads, member resistance and system capacity. For example, Fig. 11 compares the reliability indices obtained for a whole set of box girder bridge analyses showing a maximum difference in the reliability index β of 0.2 when the reliability analyses are performed with $T_r = 0.03$ s and $T_r = 0.1$ s.

9. Summary

The procedure presented in this section demonstrates the feasibility of calibrating incremental progressive collapse analysis criteria to meet a reliability target. The target reliability can be extracted from a risk analysis that considers the cost, economic and other consequences of bridge collapse accounting for the historic performance of bridges that have been subjected to significant damage. Progressive collapse analysis guidelines can then either specify the target reliability that different bridge types should meet to reduce the risk of progressive collapse and allow the engineer to select the appropriate Incremental Load Factor, ILF , from a set of curves similar to those shown in Figs. 11 and 12, or else directly specify the Incremental Load Factor, ILF , that the engineer should use in different situations. Given the target ILF value, the engineer can then execute a pushdown analysis and verify that the bridge will not fail before the incremented live load reaches that target.

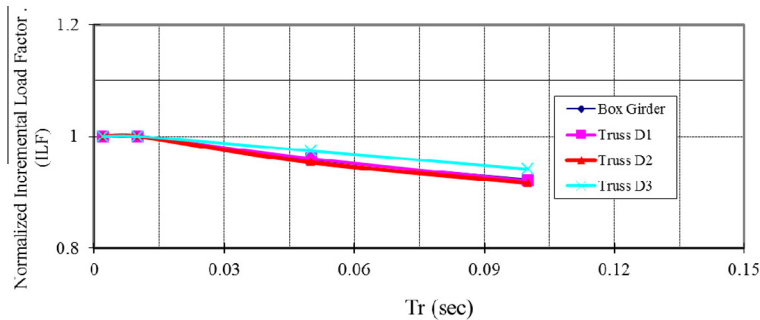


Fig. 13. Effect of impulse rise time T_r on Dynamic Load Factor.

10. Conclusions

This paper described a procedure to evaluate the reliability of bridge systems and perform a probabilistic analysis of progressive collapse should a member be suddenly damaged due to the occurrence of an external hazard.

The analysis process was illustrated using two typical bridge configurations: A two-box steel girder bridge and a steel truss bridge. The box girder bridge is assumed to be susceptible to fatigue fracture at the midspan of one box and the truss is assumed to lose the load carrying capacity of a main strut. These particular damage scenarios are selected because these two bridge types have been designated by the US Federal Highway Administration (FHWA) as non-redundant, fracture-critical configurations that are expected to collapse under their own weights if one of their members is fractured.

Statistical models for the behavior of main bridge members were primarily extracted from those used during the code calibration efforts of the AASHTO LRFD and the AISC LRFD manual of steel construction. Additional data were extracted from the literature to model the behavior of the bolts and gusset plates at the truss connections.

The live load model used in this study was based on site-specific truck weight and traffic data collected using Weigh-In-Motion (WIM) systems at a site in central New York State.

Because performing reliability analyses are beyond the day-to-day practice of bridge engineers, a methodology is presented that can be used to calibrate reliability-based criteria to help bridge engineers perform traditional incremental analyses to assess the ability of a bridge system to mitigate disproportionate collapse if one main component is subjected to sudden damage.

The reliability-calibration of the incremental progressive analysis criteria was illustrated for different damage scenarios involving the loss in the load carrying capacity of a single member of the truss bridge configuration or the fracture of the bottom flange and two webs at the midspan of the box girder bridge. The results indicate that: if a push down analysis of these bridges in their damaged configurations demonstrates an ability to sustain their dead loads and about 1.83 times the weight of two side-by-side typical US legal trucks, then they should be able to resist progressive collapse with a reliability index on the order of $\beta_{progressive} = 1.5$. A reliability index $\beta_{progressive} = 0.80$ is achieved when the incremental load factor is between 1.45 and 1.63 with an average value $ILF = 1.55$.

Future research should compare the results obtained in this paper to those from the analysis of additional bridge configurations and various damage scenarios that could include simultaneous failures in several members. Risk assessment methods and cost benefit analyses should be developed to help establish the target reliability levels that bridges susceptible to sudden local damage should achieve so that local damage would not lead to unacceptable high probability of progressive collapse.

References

- [1] ASCE-7. Minimum design loads for buildings and other structures. Virginia: American Society of Civil Engineers; 2010.
- [2] Buscemi N, Marjanishvili S. SDOF model for progressive collapse analysis. *Struct Cong* 2005;1–12.
- [3] EC 0. Basis of structural design. Belgium: Comité Européen de Normalisation (CEN); 2002.
- [4] EC 1-7. General actions – accidental actions. Belgium: Comité Européen de Normalisation (CEN); 2006.
- [5] FEMA 426. Reference manual to mitigate potential terrorist attacks against buildings. Washington (DC): Federal Emergency Management Agency; 2003.
- [6] GSA. Progressive collapse analysis and design guidelines for new federal office buildings and major modernization projects. Washington (DC): Office of Chief Architect; 2013.
- [7] DoD. DoD minimum antiterrorism standards for buildings. Washington (DC): U.S. Army Corps of Engineering; 2002.
- [8] Marjanishvili SM. Progressive analysis procedure for progressive collapse. *J Perform Constr Facil ASCE* 2004;79–85.
- [9] Ellingwood BR. Abnormal loads and disproportionate collapse: risk mitigation strategies. *Struct Cong ASCE* 2009;1–8.
- [10] Xu G, Ellingwood BR. Probabilistic robustness assessment of pre-northridge steel moment resisting frames. *J Struct Eng* 2011;137(9):925–34.
- [11] Starossek U. Progressive collapse of structures. London: Thomas Telford Publishing; 2009.
- [12] Frangopol DM, Curley JP. Effects of damage and redundancy on structural reliability. *J Struct Eng* 1987;113(7):1533–49.
- [13] Ghosn M, Moses F. Redundancy in highway bridge superstructures, NCHRP Report 406. Washington (DC): Transportation Research Board, The national Academies; 1998.
- [14] Kima J, Kimb T. Assessment of progressive collapse-resisting capacity of steel moment frames. *J Constr Steel Res* 2009;65(1):169–79.
- [15] McKay MD, Beckman RJ, Conover WJ. A comparison of three methods for selecting values of input variables in the analysis of output from a computer code. *Am Stat Assoc* 1979;21(2):239–45.
- [16] Iman RL, Davenport JM, Zeigler DK. SAND79-1473: Latin hypercube sampling (program user's guide). Albuquerque: Risk Assessment and Systems Modeling Department, Sandia National Laboratories; 1980.
- [17] Au SK, Beck JL. Estimation of small failure probabilities in high dimensions by subset simulation. *Probab Eng Mech* 2001;16:263–77.
- [18] Koutsourelakis PS, Pradlwarter HJ, Schueller GI. Reliability of structures in high dimensions, part I: algorithms and applications. *Probab Eng Mech* 2004;19(4):409–17.
- [19] Miao F, Ghosn M. Modified subset simulation method for reliability analysis of structural systems. *Struct Saf* 2011;33(4–5):251–60.
- [20] Miao F. Reliability-based progressive collapse and redundancy analysis of bridge systems (Ph.D. Dissertation). New York: Department of Civil Engineering, The City College and the Graduate Center of the City University of New York; 2013.
- [21] AASHTO LRFD Bridge Design Specifications. Washington, DC: Association of State Highway and Transportation Officials; 2012.
- [22] Hovell CG. Evaluation of redundancy in trapezoidal box girder bridges using finite element analysis (Master Dissertation). Texas: The University of Texas at Austin; 2007.
- [23] Nowak AS. Calibration of LRFD Bridge Design Code, NCHRP Report 368. Washington (DC): National Academy Press; 1999.
- [24] Hambly EC. Bridge deck behavior. London: Chapman and Hall; 1991.
- [25] Wang N, Ellingwood BR, Zureick A. Bridge rating using system reliability assessment. II: improvements to bridge rating practices. *J Bridge Eng* 2011;16:863–71.
- [26] Ghosn M, Yang J. Bridge system safety and redundancy, NCHRP Report 776. Washington DC: National Academy Press; 2014.
- [27] Holt R, Hartmann J. Adequacy of the U10 gusset plate design for the Minnesota bridge No.9340 (I-35W over the Mississippi River)-Final Report. Washington (DC): Federal Highway Administration, Turner-Fairbank Highway Research Center; 2008.

- [28] Ellingwood BR, Galambos TV, MacGregor JG, Cornell CA. Development of a probability based load criterion for American national standard A58, NBS Special Publication 577. Washington (DC): U.S. Dept of Commerce; 1980.
- [29] Galambos TV, Ravindra MK. Properties of steel for use in LRFD. *J Struct Div ASCE* 1978;104(9):1459–68.
- [30] Johnson BG, Opila F. Compression and tension tests of structural alloys. *ASTM Proc.* 1941;41:552–70.
- [31] Julian OG. Synopsis of first progress report of committee on safety factors. *J Struct Div ASCE* 1957;83(4):1–22.
- [32] Tall L, Alpsten GA. On the scatter of yield strength and residual stresses in steel members, symp. on concepts of safety of structures and methods of design. IABSE; 1969. p. 151–63.
- [33] Doane JF. Inelastic instability of wide-flange steel beams. Austin: University of Texas; 1969.
- [34] Melchers RE. Structural reliability analysis and prediction. 2nd ed. New York: Wiley; 1999.
- [35] Fisher JW, Galambos TV, Kulak GL, Ravindra MK. Load and resistance factor design criteria for connectors. *J Struct Div ASCE* 1978;104(9):1427–41.
- [36] Fisher JW, Kulak GL. Tests of bolted butt splices. *J Struct Div ASCE* 1968;94(11):2609–22.
- [37] Rumpf JL, Fisher JW. Calibration of A325 bolts. *J Struct Div ASCE* 1963;89(6):215–34.
- [38] Wallaert JJ, Fisher JW. Shear strength of high-strength bolts. *J Struct Div ASCE* 1965;91(3):99–126.
- [39] Kulak GL, Fisher JW, Struik HA. Guide to design criteria for bolted and riveted joints. 2nd ed. New York: John Wiley & Sons; 1987.
- [40] Rex CO, Easterling WS. Behavior and modeling of a bolt bearing on a single plate. *J Struct Eng* 2003;129(6):792–800.
- [41] Kim HJ, Yura JA. The effect of ultimate-to-yield ratio on the bearing strength of bolted connections. *J Constr Steel Res* 1999;49:255–69.
- [42] Fisher JW, Struik HA. Guide to design criteria for bolted and riveted joints. New York: Wiley; 1974.
- [43] AISC. Load and resistance factor design specifications for structural steel buildings (LRFD). Chicago: American Institute of Steel Construction; 2010.
- [44] Gerard G, Becker H. Handbook of structural stability, Part I-buckling of flat plates, Tech. Note 3871. Washington (DC): National Advisory Committee for Aeronautics; 1957.
- [45] Hall DH. Proposed steel column strength criteria. *J Struct Div ASCE* 1981;107:649–70. ST4 (April 1981).
- [46] Ghosn M, Sivakumar B, Miao F. Development of state-specific load and resistance factor rating method. *J. Bridge Eng.* 2013;18(5):351–61.
- [47] Sivakumar B, Ghosn M, Moses F. Protocols for collecting and using traffic data in bridge design, NCHRP Report 683. Washington (DC): Transportation Research Board; 2011.
- [48] AASHTO MBE. Manual for bridge evaluation. 2nd ed. Washington DC: Association of State Highway and Transportation Officials; 2001.
- [49] Ghosn M, Moses F, Frangopol DM. Redundancy and robustness of highway bridge superstructures and substructures. *J Struct Infrastruct Eng* 2010;6(1&2):257–78.
- [50] Samaras V, Sutton J, Williamson E, Frank K. Simplified method for evaluating the redundancy of twin steel box-girder bridges. *J Bridge Eng* 2012;17(3):470–80.